NMR and X-ray Diffraction Studies of Phases in the Destabilized LiH-Si System

R. C. Bowman, Jr.[1], S.-J. Hwang[2], C. C. Ahn[3], and J. J. Vajo[4]

[1] Jet Propulsion Laboratory, California Institute of Technology, Pasadena, CA 91109, U.S.A.

[2] Division of Chemistry and Chemical Engineering, California Institute of Technology, Pasadena, CA 91125, U.S.A.

[3] Division of Engineering and Applied Science, California Institute of Technology, Pasadena, CA 91125, U.S.A.

[4] HRL Laboratories, LLC, Malibu, CA 90265, U.S.A.

ABSTRACT

Hydrogen absorption and desorption isotherms have been measured on ballmilled mixtures of LiH+Si powders to evaluate the thermodynamics parameters of these reversible reactions. The phase compositions at the various stages of reaction have been examined by Magic Angle Spinning-Nuclear Magnetic Resonance (MAS-NMR) of the ^{7}Li, ^{1}H, and ^{29}Si isotopes and powder x-ray diffraction (XRD). The initial mixtures of LiH and Si were found to convert into known Li-Si silicide intermetallics (i.e., $Li_{12}Si_7$, Li_7Si_3, and $Li_{13}Si_4$) as well as providing evidence for a previously unknown ternary Li-Si-H phase as hydrogen was first desorbed and then absorbed. While the absorption reactions are certainly reversible over portions of the Li-Si-H composition range, incomplete recovery of the original LiH + Si phases was also observed under some test conditions.

INTRODUCTION

In order to meet U.S. DOE hydrogen storage goals proposed for years 2005 and 2010, metal hydrides will need to be mainly composed of light elements (i.e., Li, B, Mg, Al, etc.) to be viable candidates. The novel approach of destabilizing hydrogen rich but strongly bound hydrides such as LiH via alloying with Si has been recently shown to be feasible [1] and thus improve substantially their potential as hydrogen storage materials in fuel cell powered vehicles. A reversible hydrogen storage capacity totaling around 5.0 wt.% has been measured with mixtures of LiH and silicon powders where this LiH+Si system that also produces a 4-to-5 order-of-magnitude increase [1] of the equilibrium pressure compared to just LiH for temperatures below 800 K. Volumetric measurements of the hydrogen absorption and desorption isotherms in the 650 K – 780 K temperature range have revealed two and three plateau regions on lightly ballmilled mixtures of 2.5LiH+Si and 4.4LiH+Si, respectively.

In general, for two components, hydride destabilization through alloy formation upon dehydrogenation involves the reaction [1]

$$nAH_x + mBH_y \leftrightarrow A_nB_m + 1/2(nx + my)H_2 \qquad (1)$$
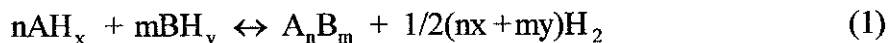
where AH_x and BH_y are binary or more complex hydrides, and n and m are specified by the stoichiometry of the AB alloy. For the LiH/Si system, a prototypical reaction would be

$$4LiH + Si \leftrightarrow Li_4Si + 2H_2 \qquad (2)$$

Because the formation of SiH_4 is endothermic, hydrogenation of Si is not expected and thus reaction 2 could be reversible. Because the Si does not hydrogenate, the Si addition reduces the gravimetric hydrogen density from that of the pure hydrides. For reaction 2, the hydrogen capacity is 6.6 wt.% compared to 12.7 wt.% for pure LiH. Since there are several Li-Si phases [2-4], which are listed in Table I along with their structure references and known NMR shifts, sequential reactions will occurred as hydrogen is desorbed from the LiH/Si mixture. The predicted hydrogen capacity for each of these reactions is also given in Table I. The objectives of the present study are to identify these lithium silicide phases and correlate their presence on the hydrogen storage properties.

EXPERIMENTAL

Lithium hydride powder and pieces of electronic-grade Si wafers were used without further purification. All sample handling was performed in an Ar filled glove box. Mixtures of LiH + Si in the ratios of 2.5:1.0 and 4.4:1.0 were prepared using mechanical milling as described by Vajo, et al. [1]. The hydrogen absorption and desorption measurements were performed using the JPL Sieverts volumetric system also described previously [1]. The hydrogen contents reported in the isotherms and used for sample compositions are arbitrarily set to zero after 8-10 hours of active evacuation while heating to the samples to at least 725 K. This procedure is used to define the reversible hydrogen capacity even though some hydrogen is retained as will be described in the following section.

The solid state Magic Angle Spinning Nuclear Magnetic Resonance (MAS-NMR) measurements were performed using a Bruker Avance 500 MHz spectrometer with a wide bore 11.7 T magnet. The resonance frequencies were 500.2 MHz for protons (^{1}H), 194.4 MHz for ^{7}Li, and 99.4 MHz for ^{29}Si. The MAS-NMR spectra were usually obtained with a 14 kHz spinning rate. The Li-Si-H samples were contained in commercial 4-mm ZrO_2 rotors with Kel-F rotor caps that had been loaded in an argon atmosphere glove box. Dry nitrogen gas was used for sample spinning. All MAS-NMR experiments were performed at room temperature. The shifts (σ) of the ^{1}H and ^{29}Si peaks are externally referenced to tetramethylsilane at 0.0 ppm and ^{7}Li peaks are relative to an external 1-molar LiCl aqueous solution at 0.0 ppm.

X-ray data were obtained with a Philips PW3040-Pro diffractometer using Cu Kα radiation and an x-ray mirror. Samples were mounted into 1 mm glass capillary tubes in an Ar glove box and sealed prior to data acquisition.

Table I. Compilation of Li-Si phases, their literature properties, and predicted hydrogen capacity

Phase	ICDD Card Number	^{7}Li σ (ppm)	^{29}Si σ (ppm)	Wt.% H_2 Stored	NMR References
Si	01-89-2749	-	-80	0.0	5
LiSi	01-87-2075	11.3	-106.5	2.8	4
$Li_{12}Si_7$	01-89-0006	-15.6	N.A.	4.1	4
Li_7Si_3	01-89-0005	N.A.	N.A.	5.0	
$Li_{13}Si_4$	01-89-0009	N.A.	N.A.	6.1	
$Li_{22}Si_5$	01-089-4228	N.A.	N.A.	7.0	
LiH	01-89-4072	N.A.	-	12.7	

N.A. = Not Available

RESULTS AND DISCUSSION

The hydrogen absorption and desorption behavior has been studied on two samples (i.e., LCS-16 and LCS-29) prepared with LiH/Si ratios of 2.5:1.0 as well as a 4.4:1.0 mixture (i.e., LCS-20). Isotherms measured near ~775 K are shown in Fig. 1, where two plateaus exist for LCS-16 and LCS-29 samples and three plateaus form for LCS-20. As stated previously [1], these plateaus reflect the presence of distinct Li_ySi_z intermetallic phases. Furthermore, the pressures for these plateaus are factors of $\sim 10^2 - 10^4$ higher than the equilibrium value (i.e., ~9.3 Pa) predicted for solid LiH at 775 K from an extrapolation of prior results [6] obtained at higher temperatures. Hence, a substantial hydride destabilization effect is observed with silicon alloying [1]. The hydrogen contents in Fig. 1 are referenced to "zero" following an overnight desorption with the samples above 750 K under active evacuation [1]. The resulting maximum reversible hydrogen capacity is ~5.5 wt.%; whereas, the total desorption from a 4.4:1.0 LiH/Si mixture would be 7.0 wt.% by forming $Li_{22}Si_5$ from eqn. 1 and Table I. To better assess these reactions and to identify the product phases, the powder XRD and MAS-NMR tests were done.

Representative XRD patterns obtained on various Li_ySiH_x samples (where y = 2.5 or 4.4 and x is defined as "0.0" after overnight evacuations and x-values between $0.77 \leq x \leq 2.9$ for the reacted samples are from volumetric measurements using the Sieverts system [1]) are given in Fig. 2. The XRD peaks of the reference compounds listed in Table I are included near appropriate measured traces in Fig. 2. The identified phases found in samples from different stages of reaction are summarized in Table II along with the final processing step for each sample. While many samples yielded the expected silicide product phases (i.e., $Li_{12}Si_7$, Li_7Si_3, and $Li_{13}Si_4$) along with LiH and Si at the appropriate hydrogen content, numerous additional XRD peaks were assigned to a previously unknown phase with an orthorhombic structure (i.e., $o\text{-}Li_ySi_zH_x$) for at least two of the samples (i.e., x = 1.0 and x = 1.4). Further evidence for this unexpected component is provided by the NMR results. However, XRD did not indicate the presence of LiSi, $Li_{22}Si_5$ or any impurity phases (e.g., complex oxides or hydroxides).
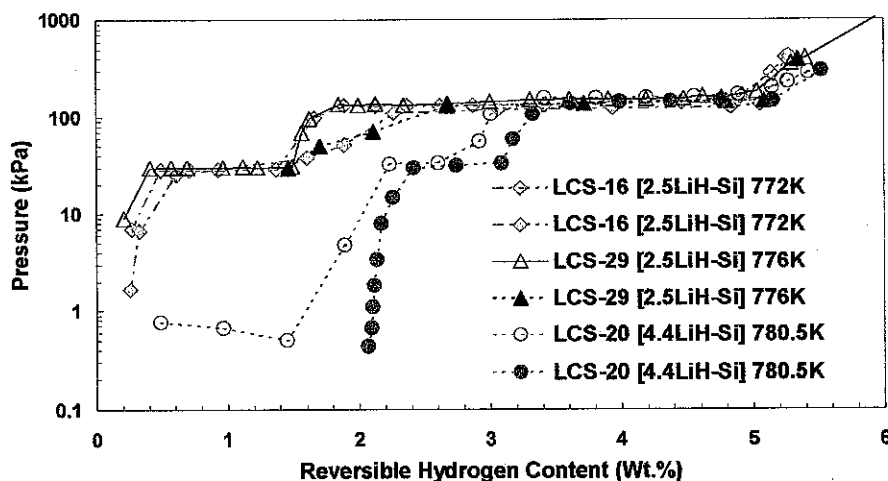

Figure 1. Hydrogen absorption (open symbols) and desorption (filled symbols) obtained near 775 K on three different samples of ballmilled LiH:Si mixed in the ratios of 2.5:1.0 for LCS-16 and LCS-29 and 4.4:1.0 for LCS-20.
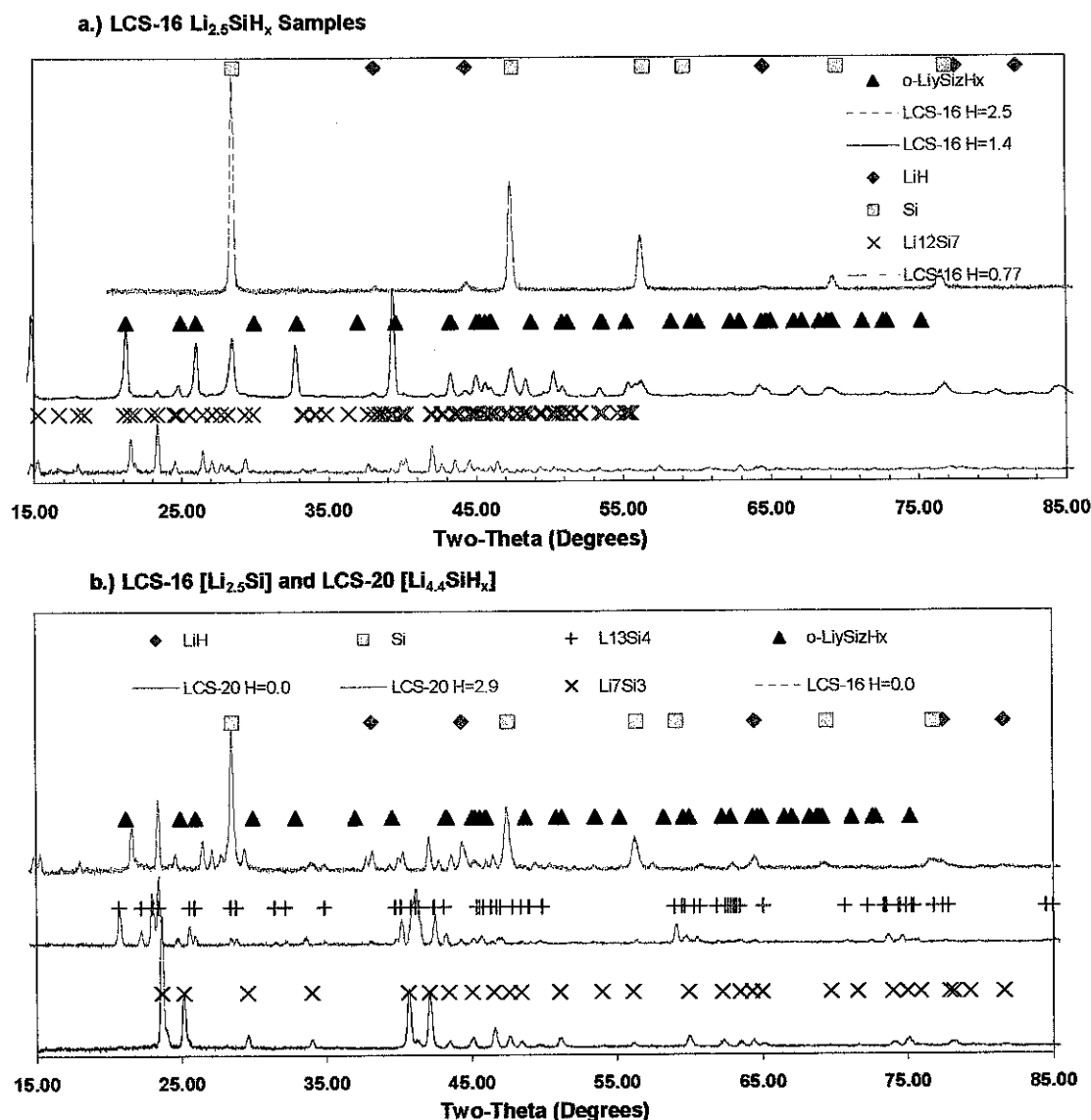
a.) LCS-16 Li$_{2.5}$SiH$_x$ Samples

b.) LCS-16 [Li$_{2.5}$Si] and LCS-20 [Li$_{4.4}$SiH$_x$]

Figure 2. Powder x-ray diffraction (XRD) patterns for several Li$_y$Si$_z$H$_x$ samples after various stages of hydrogen absorption and desorption.

Table II. Phase Compositions for Li$_y$SiH$_x$ samples from XRD and NMR measurements.

Lot ID	Last Treatment	x	XRD Phases Found	NMR Phases Found
LCS-16	As ballmilled	2.5	Si, LiH	LiH, Si
LCS-16	Desorb overnight @ 755K	0.0	Li$_7$Si$_3$	Li$_7$Si$_3$
LCS-16	H$_2$ absorbed @ 746K	0.77	Li$_{12}$Si$_7$, LiH	Li$_{12}$Si$_7$, LiH
LCS-16	Desorbed @ 755K	1.0	o-Li$_y$Si$_z$H$_x$, Si, LiH	o-Li$_y$Si$_z$H$_x$, LiH, Li$_{12}$Si$_7$
LCS-16	Desorb @ 725K	1.4	o-Li$_y$Si$_z$H$_x$, LiH, Si	o-Li$_y$Si$_z$H$_x$, LiH
LCS-20	Desorb overnight @ 780K	0.0	Li$_{13}$Si$_4$, LiH	Li$_{13}$Si$_4$, LiH
LCS-20	H$_2$ absorb @ 723K	2.9	Si, LiH, o-Li$_y$Si$_z$H$_x$(?)	LiH, Li$_{12}$Si$_7$, ?
LCS-29	H$_2$ absorb @ 774K	2.3	Si, LiH, ?	LiH, Si

The MAS-NMR spectra of ^{1}H, ^{7}Li, and ^{29}Si spins from five LCS-16 samples with differing H-contents are presented in Fig. 3a,b,c, respectively. The ^{29}Si spectra for other compositions of the LCS-20 and LCS-29 samples are shown in Fig 3d. The prominent spinning side bands are evident in Fig. 3a for the protons in LiH and reflect the strong ^{1}H-^{1}H homogenous dipolar coupling in this compound. All the spin-lattice relaxation times (T_1) are very long (i.e., ~1-3 hours) for LiH and Si while the T_1 values of the ^{7}Li and ^{29}Si spins are much shorter (i.e., only ~1-10 s) for the lithium silicide phases. Hence, vastly different pulse repetition rates (d1) were necessary to observe signals from all phases present in a specific sample. This situation has impeded quantitative determinations of relative phase contents – for example, the presence of crystalline Si in the LCS-16 x=1.4 and 1.0 samples is missing in Fig. 3c because d1 was only 2s. Without performing detailed analyses but correlating NMR peaks with the XRD results, the following peak shift σ assignments have been made for the various $Li_ySi_zH_x$ phases: LiH (^{1}H=3 ppm; ^{7}Li=0 ppm); Si (^{29}Si= -81 ppm); $Li_{12}Si_7$ (^{7}Li=21 ppm, 16 ppm, -17 ppm; ^{29}Si=303 ppm, 283 ppm, 220 ppm, 170 ppm, 60 ppm); Li_7Si_3 (^{7}Li=14 ppm; ^{29}Si=310 ppm); $Li_{13}Si_4$ (^{7}Li=23 ppm, 9 ppm; ^{29}Si=293 ppm, 258 ppm); and o-$Li_ySi_zH_x$ (^{1}H=40 ppm, ^{7}Li=10 ppm, ^{29}Si ~179-183 ppm). The last assignments for the previously unknown o-$Li_ySi_zH_x$ phase is mainly based on the absence of these peaks in other possible phases such as LiSi [4], amorphous silicon [5,7], and the chemical shifts for different Si-Si and Si-O coordinations [7]. The phase compositions deduced from the MAS-NMR spectra in Fig. 3 are listed in the last column of Table II. Very consistent matching of phase identities from the MAS-NMR and XRD assignments was achieved for nearly all the samples where the only residual ambiguities are for samples LSC-20 with x = 2.9 and LSC-29 with x = 2.3. These samples are being more thoroughly characterized to resolve their correct and complete phase compositions.

As summarized in Table II, the sequential formation of lithium silicide phases with increasing silicon concentration occurs as more hydrogen is desorbed from the ballmilled mixtures of LiH and Si. However, both XRD and NMR clearly demonstrated the significant LiH remains in sample LCS-20 that had been thoroughly desorbed by active pumping for many hours while the material was continually heated at ~780 K. Hence, complete conversion into $Li_{22}Si_5$ did not occur, which resulted in a reduced reversible hydrogen storage capacity that was about 2 wt.% lower than was predicted in Table I for this final product phase. Presumably, higher temperatures and more efficient hydrogen removal beyond present capabilities would be needed. This behavior indicates a possible limiting condition for the hydride destabilization effect [1]. The occurrence of currently unidentified o-$Li_ySi_zH_x$ phase implies that for some experimental conditions the destabilized hydrogen absorption/desorption reactions are not entirely reversible although most of the samples appear to follow the general reaction reactions given by eqn. 1. Further assessments into the details of o-$Li_ySi_zH_x$ phase are in progress to determine its composition and structure as well as better understand the overall destabilization processes.
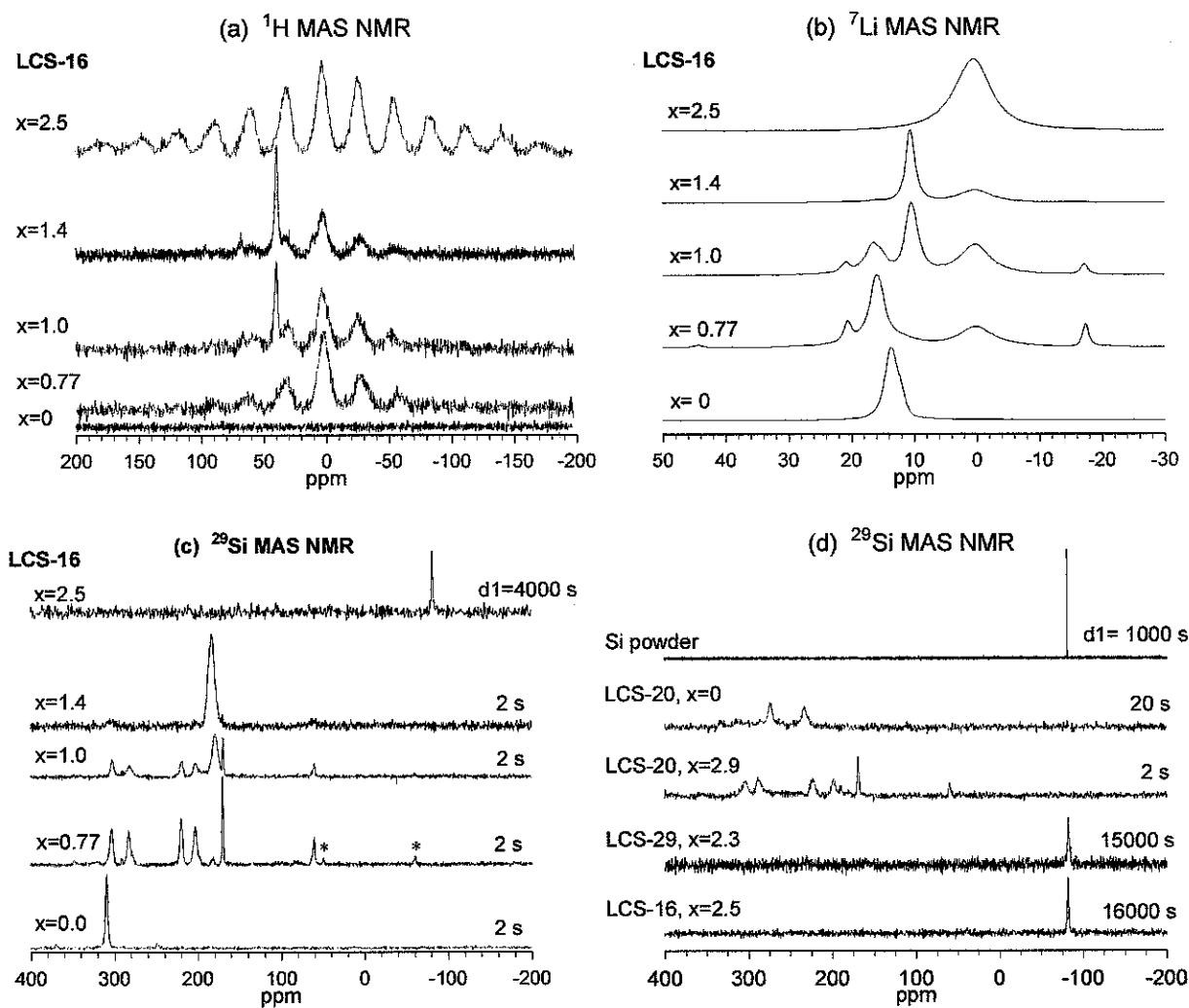
ACKNOWLEDGMENTS

Figure 3. MAS-NMR spectra for various samples of Li_ySiH_x where y=2.5 for samples LCS-16 and LCS-29 and y=4.4 for LCS-20 samples. "*" denotes spinning side band peaks in the spectra.

REFERENCES

1. J. J. Vajo, F. Mertens, C. C. Ahn, R. C. Bowman, Jr., and B. Fultz, *J. Phys. Chem.* **B108**, 13977 (2004).
2. C. van der Marel, G. J. B. Vinke, and W. van der Lugt, *Solid State Comm.* **54**, 917 (1985).
3. M. H. Braga, L. F. Malheiros, and I. Ansara, *J. Phase Equil.* **16**, 324 (1995).
4. L. A. Stearns, J. Gryko, J. Diefenbacher, G. K. Ramachandran, and P. F. McMillan, *J. Sol. St. Chem.* **173**, 251 (2003).
5. W.-L. Shao, J. Shinar, B. C. Gerstein, F. Li, J. S. Lannin, *Phys. Rev. B***41**, 9491 (1990).
6. E. Veleckis, *J. Nucl. Mater.* **79**, 20 (1979).
7. M. S. Brandt, S. E. Ready, and J. B. Boyce, *Appl. Phys. Lett.* **70**, 188 (1997).